[i]Tomografia para a determinação da distribuição espacial do Vapor de Água através de observações GNSS

Tomographic determination of the spatial Distribution of Water Vapor using GNSS observations

André Sá [1,2], Fábio Bento [2], Rui Fernandes [2], Paul Crocker [2]
[1]UDI/IPG, Av. Dr. Francisco de Sá Carneiro, 50 6300-654 Guarda, Portugal, andre_sa@ipg.pt
[2]SEGAL (UBI/IDL), R. Marquês d'Avilla 6201-001 Covilhã, Portugal, fbento@segal.ubi.pt, rmanuel@di.ubi.pt, crocker@di.ubi.pt

SUMMARY

This paper focuses on investigating Global Navigation Satellite Systems (GNSS) observations as precipitation sensors and also analyse the contribution of the GNSS dense networks as an efficient tool for meteorological purposes based on Water Vapor Tomography. For that, case-studies are presented using data from BELEM and MANAUS dense network. For Water Vapor Tomograhy, a software package has been developed to reconstruct the GNSS water vapour spatial distribution. The obtained results indicate that GNSS can detect the variations in precipitation at different periods of the year and that dense GNSS networks allow us to generate images of the spatial and temporal distribution of water vapour. However, the influence of several parameters, such as number and distribution of receivers, grid sizes and initial values, has to be taken into account for the image reconstruction.

1. INTRODUCTION

Humankind has been trying to predict the weather for millennia and always recognized importance of better understanding the weather and climate by monitoring it´s major parameters. In this respect, water vapor plays a major role in many atmospheric processes concerning physics, thermodynamics and dynamics. The knowledge of the spatial and temporal distribution of water vapor in the lower atmosphere (troposphere) is crucial for accurate quantitative prediction of precipitation and better understanding of many atmospheric processes like deep convective events.

Studies about the use of GNSS observations with focus on meteorology started about 20 years ago [Bevis et al., 1992]. GNSS has large advantages since it is a system that works under all weather conditions, with continuous unattended operation, good time resolution and an ever increment in the number of stations at many regions. GNSS observations are nowadays a well-establish tool to measure the water vapor content in the lower atmosphere. In this paper the main objective is to ascertain the sensitivity of GNSS receivers for atmospheric water vapor and contribution for meteorological purposes through several analyses, namely: Zenith Total Delay (ZTD) analyses, Precipitable Water Vapor (PWV) analyses and finally, water vapor image reconstruction applying tomography techniques using GNSS dense networks.

2. DESCRIPTION AND METHODOLOGY

While travelling through the Earth's atmosphere the GNSS signal is going to experience delays caused by the atmosphere, mainly ionosphere and troposphere. Considering the dispersive character of the ionosphere for the GNSS frequencies, ionospheric effects are minimized using a fitted linear combination of the GNSS frequencies [Brunner and Gu, 1991]. Conversely, the tropospheric effects are not frequency dependent below 15 GHz. The main effect of the troposphere on GNSS, is an extra delay of the radio signal emitted by GNSS satellites [Davis et al., 1985]. This delay is time varying due to the variable pressure, temperature and water vapor content of the atmosphere and cannot be modeled or predicted with sufficient precision positioning, especially in real-time. In figure 1 the S represents the curved path of the radio signal transmitted from the satellite to the receiver on the ground and G is the straight line distance that would have been the path without any atmosphere (vacuum). The excess propagation time of GNSS signal is the difference between both.

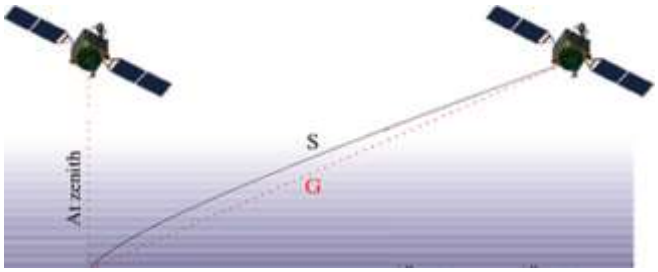

Figure 1 – Effect of the atmospheric refraction on GNSS signal propagation (Source: http://gnss.be/troposphere_tutorial.php)

In order to obtain accurate positions, the effect of the troposphere delay needs to be properly estimated. This is done by computing tropospheric parameters during the GNSS data analysis: Zenith Tropospheric Delay (ZTD) and Horizontal Gradients [Bar-Sever, 1998]. The correlation between these delays and the state of the atmosphere has been studied in order to ascertain the GNSS system as an efficient tool for meteorological observations. Most of the scientific software packages (e.g., GIPSY-OASIS, BERNESE, and GAMIT) permit to estimate the ZTD, from which the PWV can be derived knowing temperature and pressure at the site location. ZTD (Figure 2) is equal to ZHD + ZWD, where the hydrostatic delay (ZHD) is the major component (90-97%) and can be accurately inferred from measurements of surface pressure. However, the other, the wet delay (ZWD), although much smaller, can have significant temporal and spatial variations. It is this component that is estimated in the GNSS processing. PWV can be derived from estimated ZWD using the following formulas, where k'_2 and k_3 are empirical physical constants, ρ is the density of liquid water, R_v is the specific gas constant for water vapor, and T_m is the surface temperature:

$$PWV = \pi * ZWD \quad (1)$$

$$\pi = 10^6 / (\rho R_v (k'_2 + \frac{k_3}{T_m})) \quad (2)$$

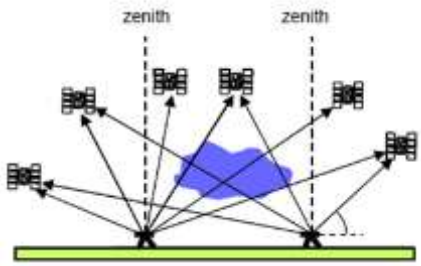

Figure 2 – Zenith Total Delay has a function of the delays for all observed satellites (Source: Van Baelen, 2009)

As the PWV is obtained from ZTD and being ZTD of any single GNSS station an estimation of the total content of the water vapor on the column above the receiver, it is impossible to compute a PWV profile from one unique station. Thus, according to this, if we have several stations it's theoretically possible to compute a PWV profile over an area. To obtain a PWV profile, a recent technique called water vapor tomography has been developed in order to compute 4D images of PWV. This technique is based on Algebraic Reconstruction Techniques (ART) and only works if there are multiple GNSS stations in a relatively small area, the designated GNSS dense networks.

ART are iterative algorithms that were initially developed with success for medical imagery. Algebraic reconstruction is an approach for image reconstruction which uses data from a series of projections such as these obtained from electron microscopy, x-ray, etc. Algebraic Reconstruction Algorithms are also useful when energy propagation paths between the source and the receiver position are the subject to ray bending on account of refraction or when energy undergoes alternation along ray paths. Description of the use of such techniques for reconstruction of water vapor spatial distribution can be found in Champollion et al. [2005] and Bender et al. [2011]. In our case, the projections are the delay on the GNSS signal path from the satellites to the receiver, the designated Slant Delays. To compute these slant delays mapping functions are used that will map the estimated ZTD for each station in the directions of the visible satellites. Troposphere tomography divides the earth´s atmosphere into small volume elements or voxels (cf. Figure 3) and uses the slant delays to estimate the refractivity of each voxel and hence get a height profile of refractivity. The output consists in 2D slices of the 3D water vapor image in latitude, longitude or altitude.

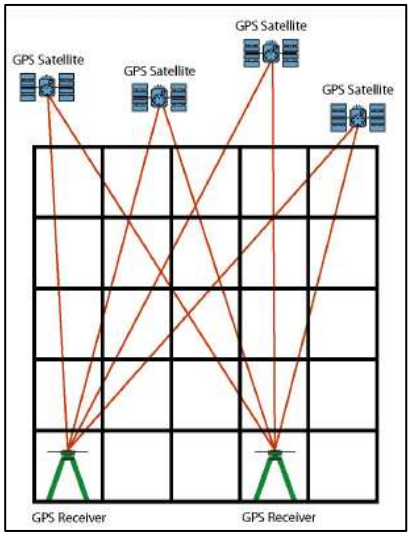

Figure 3 – The refractivity in the atmosphere along raypath of a GPS satellite signal to a ground-based receiver is discretized by a 3D voxel model (Source: Van Baelen, 2009)

For this purpose a software package, SEGAL GNSS WAter Vapor Reconstruction Image Software (SWART), has been developed at Space and Earth Analyses Laboratory (SEGAL). This package currently consists of four C++ programs that gather the necessary information to compute the Integrated Water Vapor (IWV)[1] distribution over a specified area using GPS observations. It can also perform the water vapor image reconstruction and plot the result in latitude, longitude and height slices.

For image reconstruction several ART were implemented and parallelized, namely: Kaczmarz, Landweber and Simultaneous Algebraic Reconstruction Technique (SART). The algorithms implemented were validated using Shepp-Logan Phantom image which is a standard image for image reconstruction tests. Tests were performed using an original image (Figure 4a) with a resolution of 80*80 and the projection data was generated using 75 parallel rays over 36 different angles. As can be seen in the Figure 4b-d all the algorithms reconstructed the original image reasonably well.

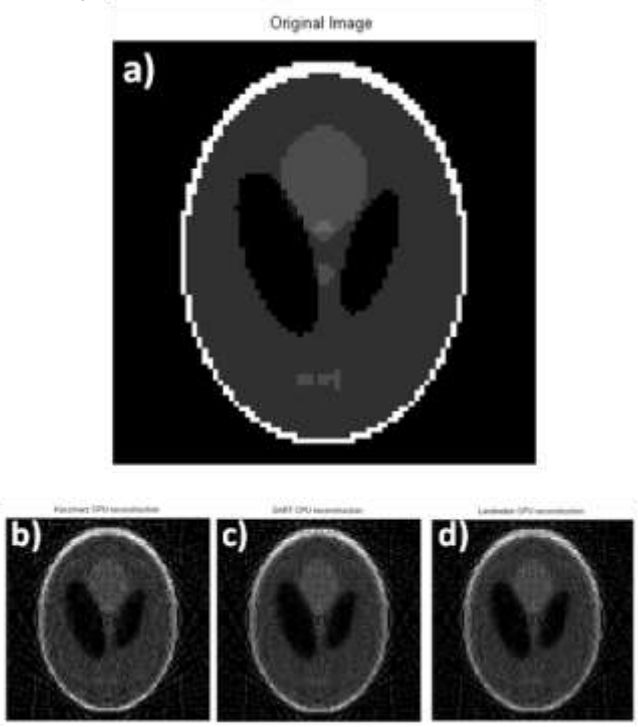

Figure 4 – a) Shepp-Logan phantom original image, b) Shepp-Logan phantom Kaczmarz reconstruction, c) Shepp-Logan phantom SART reconstruction, and d) Shepp-Logan phantom Landweber reconstruction

The standard deviation (std) of the residuals was calculated for each reconstruction. The max (z max) and min (z min) of the residuals were also calculated. The results are presented in Table 1.

Table 1 **– Standard deviation of the residuals**

ART	Std	zmin	zmax
Kaczmarz	0.116	-0.474	0.639
Landweber	0.122	-0.470	0.692
SART	0.114	-0.467	0.651

All the tested algorithms obtained similar results, all being suitable for the intended purpose.

[1] IWV is used when we state the mass of water per unit area, and Precipitable Water Vapor (PWV) if we refer to the height of an equivalent column of water, PWV = IWV/ ρ

To validate SWART results, but now using the GNSS observations, SWART was firstly tested with synthetic data and the results were compared with the results computed by LOFFT_K using the same data [Champollion et al., 2005]. LOFTT_K is a GNSS water vapor tomography software developed at Montpellier University in the Laboratoire Dynamique de la Lithosphere.

Main differences between softwares can be summarized as follows: LOFFT_K was written in Fortran language while SWART has been developed in C++; LOFFT_K implements a Kalman filter which allows the program to take into account the rapid or slow variation of the water vapor in the atmosphere, while SWART doesn´t implement a Kalman filter yet. However the main difference between both softwares consist in the matrix inversion scheme. While LOFTT_K uses the Single Value Decomposition method, SWART uses parallel algebraic reconstruction algorithms (ART). ARTs have several advantages over other methods for the water vapor tomography (Bender et al., 2011), as they perform better when energy propagation paths between the source and the receiver position are subject to ray bending on account of refraction or when energy undergoes alternation along ray paths as already mentioned.

For the comparison tests between these softwares synthetic slant (artificial) wet delays and real data (i.e satellite and receivers positions) from the ESCOMPTE campaign [Champollion et al., 2005] were used (Figure 5). Regarding the SWART software the three ART were used and the results plotted for the same latitudes and longitude slices. Results were then compared with results obtained with LOFTT_K (Figure 6). Despite the mentioned differences between softwares, it is possible to see that both softwares retrieve generically similar results (Figure 6ab). The SWART image does not seem to be smooth as the LOFFT_K image, this may be a consequence of not using kalman filter. The values of the density of the water are approximately the same for both figures.

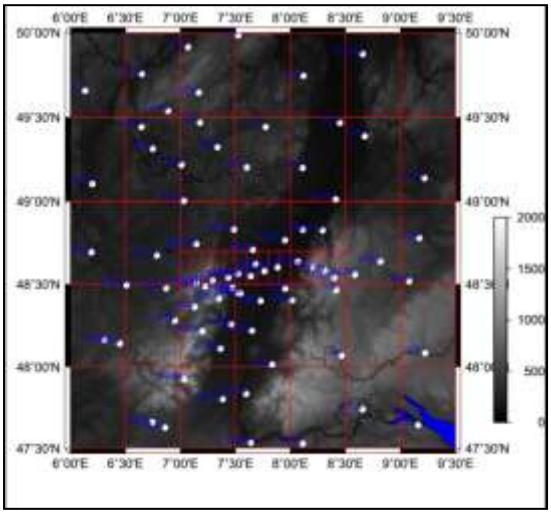

Figure 5 – 85 GNSS receivers from ESCOMPT campaign

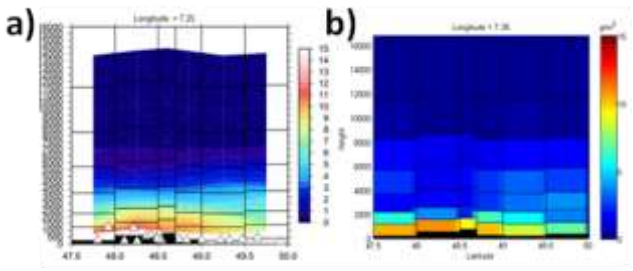

Figure 6 – Image reconstruction for slice long=7.25 a) LOFFT_K and b) SWART_KACZMARZ.

Quantification of the differences between the results from the two software's was computed as can be seen in Figure 7a-c.

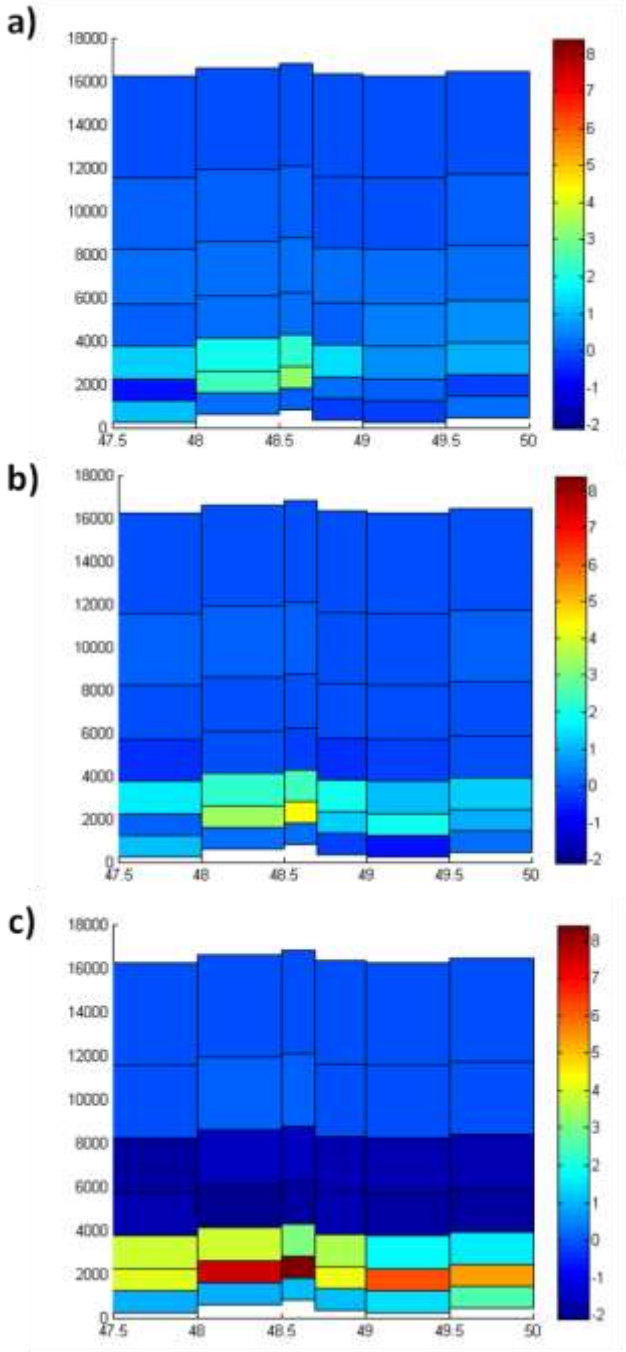

Figure 7 – Differences obtained between LOFFT_K and a) SWART (KACZMARZ), b) SWART (SART) and c) SWART (LANDWEBER)

From the differences analysis it was possible to identify that Kaczmarz and SART ARTs retrieved similar results between them, and comparable to LOFFT_K results Figure 7a-b, while Landweber appeared higher differences Figure 7c.

3. STUDIES and RESULTS

Several case studies carried out concerning the application of GNSS observation for weather and climate monitoring are here presented. The first study accesses the reliability of ZTD estimates,

and consequently, the derived PWV values. The second example shows the use of PWV estimates at single stations to evaluate the correlation of temporal variations of PWV with precipitation. Finally, some tests and results using SWART are presented. The examples are based on data from two dense GNSS networks installed in Brazil with the collaboration of SEGAL: Manaus and Belem. The data from Manaus network (Figure 8) were acquired during more than one year and the data in Belem were acquired in the framework of CHUVA project [Adams et al., 2011] during September, 2011 (Figure 9). For the different periods the PWV were computed and compared with Precipitation. As there are meteorological stations collocated with these GNSS networks that allow us to have precise values for surface temperature and pressure.

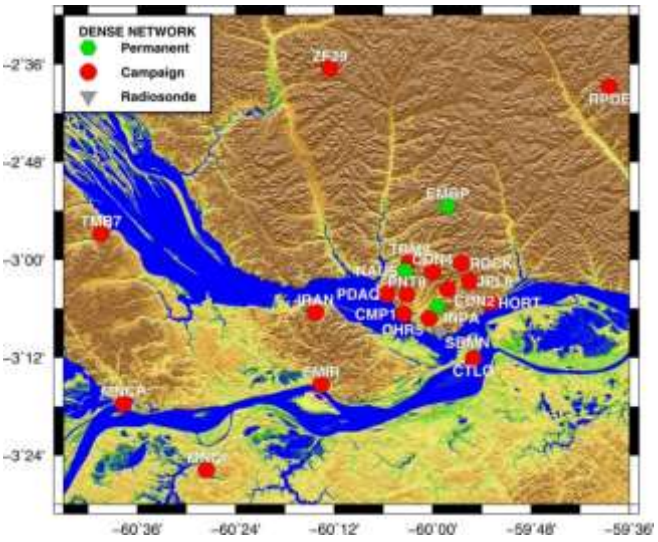

Figure 8 – MANAUS GNSS dense network, composed by Permanent stations, Campaign stations and a Radiosonde station

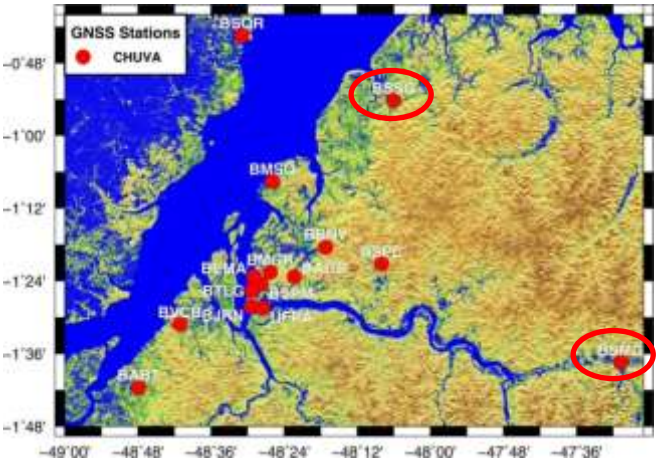

Figure 9 – BELEM GNSS dense network, stations from CHUVA project

3.1 SENSITIVITY OF GNSS TO ZTD VARIATIONS

Figure 10 shows the ZTD for seven GNSS stations from BELEM GNSS network for one day. It is possible to observe that the BSMG and the BSSG sites present the most different patterns of ZTD variation through time. Spatially these stations are the ones farthest apart from the rest of the core network (cf. Figure 9). The closer the stations the most similar ZTD patterns are observed. These results reveal the sensitivity of the GNSS observations to Water Vapor.

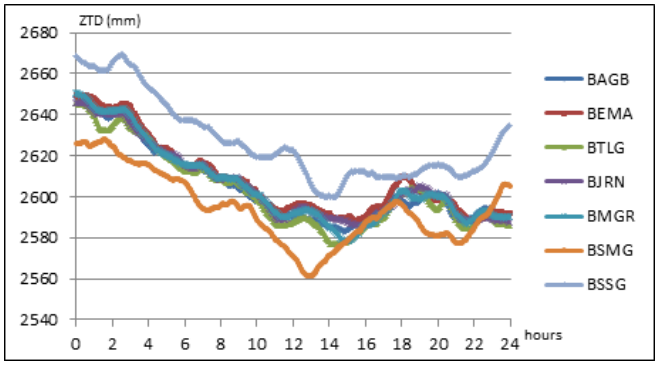

Figure 10 – ZTD from 7 stations of BELEM network for the 1st June 2011.

3.2 PWV and PRECIPITATION

For small periods, the correlation between PWV and Precipitation is not so obvious, as it can be observed in Figures 11 and 12 that show representative days for INPA station (Manaus network). Nevertheless, it is observed that relative high values of PWV correspond to high values of precipitation. However, sometimes there is a delay between peaks in both parameters, which may be caused by the fact that not all water vapor on the atmosphere is converted into rain. It is also observed that large increases followed by a decrease in PWV can correspond to occurrence of precipitation. Further tests will be performed to infer on the possibility of using the PWV variation to identify rainfall patterns.

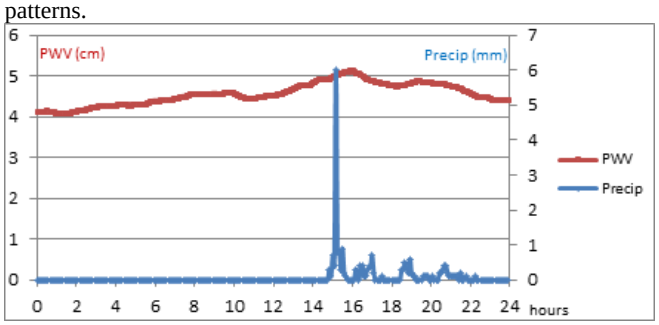

***Figure 11* – INPA station: Comparison between PWV and Precipitation for the 5th January, 2011**

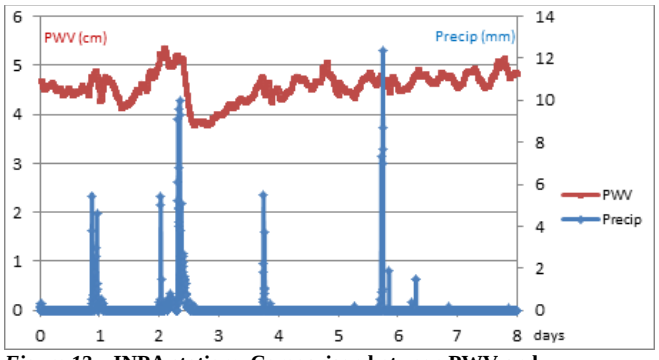

***Figure 12* – INPA station: Comparison between PWV and Precipitation for 8 days (1st/ 8th of March, 2011).**

3.3 WATER VAPOR TOMOGRAPHY

After validating SWART (see description and methodology section), some tests regarding the grid size coverage, number of receivers and initialization values for the same image reconstruction were conducted.

3.3.1 Initialization tests

For the first test the influence of the initialization values and number of iterations was checked using data from ESCOMPT campaign. Comparing the results for the same slice (Long=7.25) between using no initialization values and 100 iterations and using 15 as initialization value under 2500 m and also 100 iterations, the differences are considerably large, as it is visible in Figures 13 and 14.

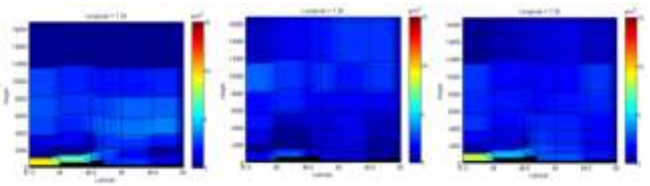

***Figure 13* – Initialization values test: Using no initialization values and 100 iterations**

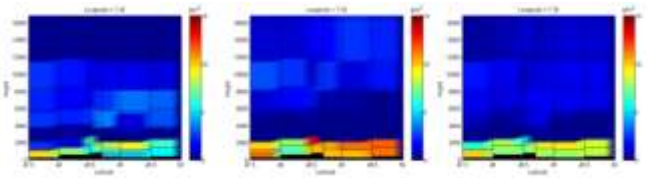

***Figure 14* – Initialization values test: Using 15 as initialization values under 2500 m and 100 iterations**

However, for the same test if the number of iterations is substantially increased for 50 000 iterations the results are similar (Figure 15 and Figure 16) and the influence of initialization values is unnoticed. It is important to mention that this test was made for an area with a good GNSS stations coverage, for other cases the results can be very different and the initialization values can have other kind of influence.

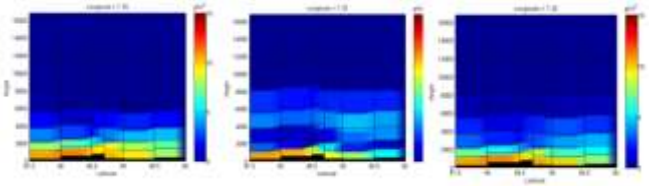

***Figure 15* – Initialization values test: Using no initialization values and 50 000 iterations**

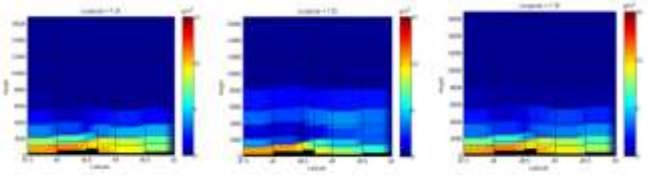

***Figure 16* – Initialization values test: Using 15 as initialization values under 2500 m and 50 000 iterations**

3.3.2 Distribution and Number of GNSS stations tests

For the second test it was analyzed the influence of the number and distribution of the GNSS receivers. It was also used the data from ESCOMPT campaign, and initially it was analyzed the influence of the GNSS receivers surrounding the study area (white square on Figure 17). For that, the image reconstruction was computed with all the 85 stations (Figure 18), and then 15 surrounding stations were removed with the particularity of trying to keep at least one station per voxel, for the final test all surrounding stations were removed, just 45 stations were used.

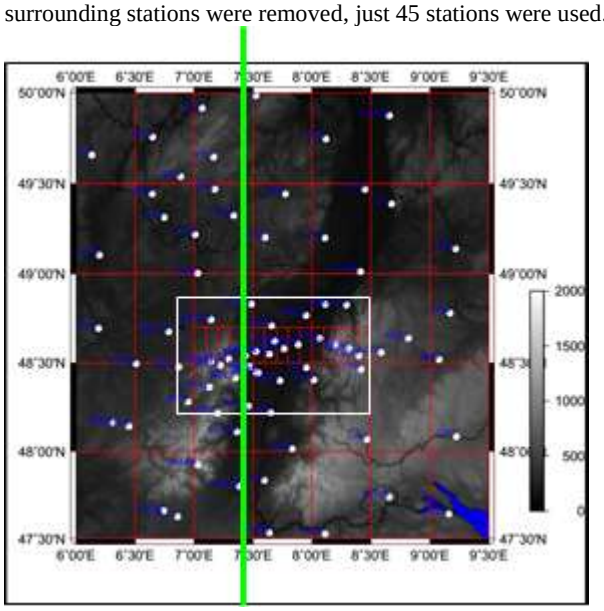

***Figure 17* – ESCOMPT campaign: Distribution of GNSS stations**

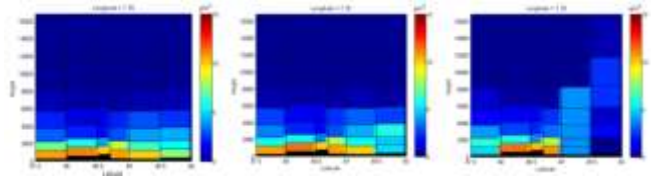

Figure 18 – Image reconstruction with a) 85, b) 70 and c) 45 stations.

To better verify the influence, the differences between the original image reconstruction (85 stations) and the other images was computed, as can be seen in Figure 19.

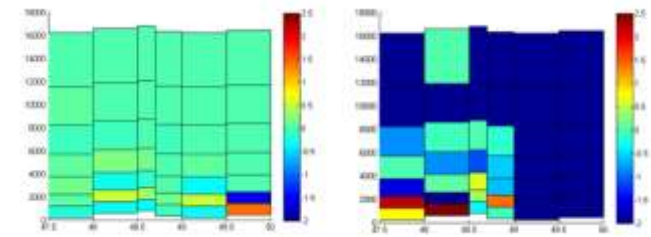

***Figure 19* – SWART diff a) 85 -70 and b) 85-45.**

Here it is shown the influence of the surrounding stations regarding a specific study area. The importance of the surrounding stations, and being few in number, lead us to think that the best way to achieve their contribution without influencing the matrix inversion with empty voxels, will be using a main dense grid for the study area and a sub grid for the surrounding area.

3.3.3 BELEM Network (Brazil) – Project CHUVA

Finally, it is presented the current status of the analysis being carried out for a dense network in Belem, Brazil with data acquired in the framework of the project CHUVA during September, 2011. GPS Data was processed using the following procedures: GIPSY/OASIS V6.2, PPP approach, VMF1 Grid mapping function, each day computed using 30h time spam (same orbits), transfer function to remove jumps between consecutive days.

For the area (red square in figure 20a) the data was processed and the image reconstruction was computed for lat=-1.35 slice (Figure 20b).

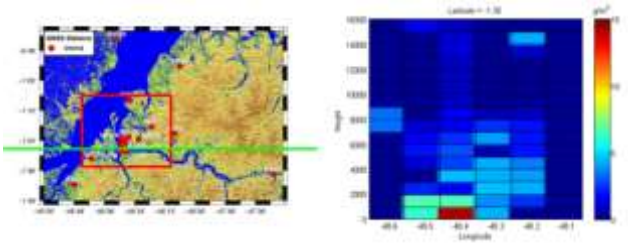

Figure 20 – a) **Study area of BELEM GNSS dense network, stations from CHUVA project*; b)* Slice lat =-1.35, vertical resolution 1000 and horizontal resolution 0.1**

Different parameterization was used for the same image reconstruction regarding the horizontal and vertical grid resolution (Figure 20b, 21a-b). The importance of both resolutions is evident, emphasizing the need to find the most appropriate resolution according to the geometry and density of the network under analysis. High grid resolution can lead to voxels with lack of information, more computational requirement and problems in inversion.

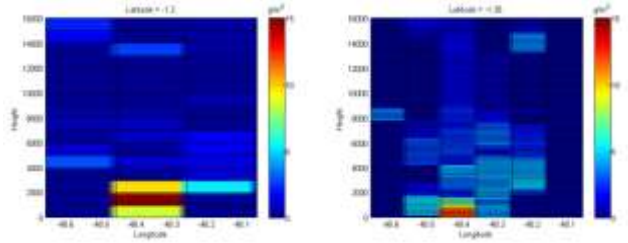

Figure 21 – a) **Slice lat =-1.35, vertical resolution 1000 and horizontal resolution 0.2, b) Slice lat =-1.35, vertical resolution 200 and horizontal resolution 0.1**

The presence of radiosondes allows the comparison of tomography results with measured data (Figure 22). Comparison reveals similar results for lower altitudes, although with some abnormal signals detected.

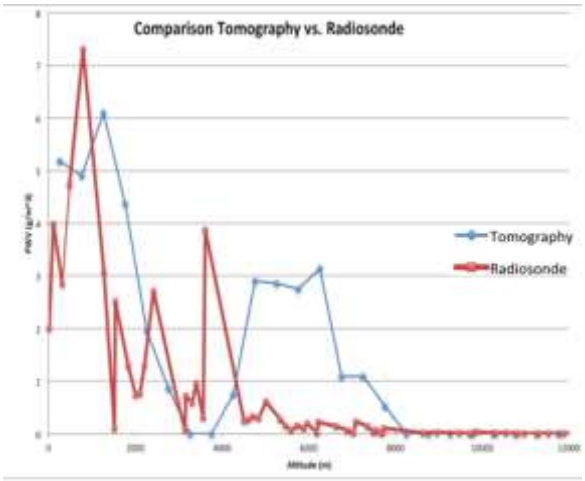

Figure 22 – PWV **comparison between Tomography and Radiosonde**

4. CONCLUSIONS

This study shows the capability of the GNSS observations as a water vapor sensor. The examples using BELEM and MANAUS data show a good agreement between the PWV variations and Precipitation. Further studies are required to identify patterns of rainfall from the GNSS-PWV time-series. We showed that the ART are valid approaches to create tomographic images with accuracy and performance

Kazmarcz and SART show better results than Landweber when compared with the solutions provided by LOFTTK

An additional advantage of these algorithms is their capacity to be paralelized which can permit their use in near real-time applications. The tomographic solutions, although sensitive to the initial values, tend to converge if sufficient number of iterations are used (the handicap is the increment in time).

Initial results for Belem show the existence of correlation with vertical profiles acquired by radiosondes even if some abnormal signals are detected. The next step is to further investigate by using more examples in order to evaluate the feasibility of using such values to constrain our derived 4D tomographic image of PWV in that campaign.

When dense GNSS networks are available, the reconstruction of 4D water vapor distribution images is feasible although this requires the use of large amount of information. These studies illustrate the beneficial aspects of GNSS for weather forecasting and that can be a great supporter in high-resolution numerical weather prediction models. Ultimate goal is that the data from these networks could be integrated in forecasting numerical models in a routinely procedure.

5. REFERÊNCIAS

Adams, D.K., R.M. Fernandes, E. R. Kursinski, J.M. Maia, L.F. Sapucci, L. A. Machado, I. Vitorello, J. Galera, K.L. Holub, S.I. Gutman, N. Filizola, R.A. Bennett (2011), A dense GNSS meteorological network for observing deep convection in the Amazon, Atmospheric Science Letters, 10.1002/asl.312

Baelen, Joel, Aubagnac, Jean-Pierre; Dabas, Alain, Comparison of Near-Real Time Estimates of Integrated Water Vapor Derived with GPS, Radiosondes, and Microwave Radiometer, Journal of Atmospheric & Oceanic Technology, Vol. 22 Issue 2, p201, Feb 2005

Bar-Sever, Y. E., and P. M. Kroger, Estimating horizontal gradients of tropospheric path delay with a single GPS receiver, J. Geophys. Res., 103, 5019±5035, 1998.

Bastin S, Champollion C, Bock O, Drobinski P, Mason F. 2007. Diurnal cycle of water vapor as documented by a dense GPS network in a coastal area during ESDCOMPTE IOP2. Journal of Applied Meteorology and Climatology 46: 167–182

Bender, M., Dick,G.,Ge, M.,Deng, Z., Wickert,J., Kahle,H.-G., Raabe, A., Tetzlaff,G.
"Development of a gnss water vapour tomography system using algebraic reconstruction techniques," Advances in Space Research, vol. 47, no. 10, pp. 1704 – 1720, 2011, GNSS Remote Sensing-2. [Online]. Available: http://¬www.sciencedirect.com/¬science/¬article/¬pii/-S0273117710003790.

Bevis, M., S.Businger, T.Herring, C. Rocken, R. Anthes and R. Ware, GPS Meteorology: Remote Sensing of the Atmospheric Water Vapor Using GPS, J. Geophys. Res., 97, 15, 787-15, 801, 1992.

Brunner, F. K., and M. Gu, "An improved model for the dual frequency ionospheric correction of GPS observations," Manuscripta Geodaetica, vol. 16, p. 205-214, 1991.

Champollion, F. Masson, M.-n. Bouin, A. Walpersdorf, E. Doerflinger, O. Bock, and J. Van Baelen, "Gps water vapor tomography: preliminary results from the escompte field experiment," Atmospheric Research, vol. 74, no. 1-4, pp. 253–274, 2005.

Davis, J. L., T. A. Herring, I. I. Shapiro, A. E. Rogers, and G. Elgered, Geodesy by radio interferometry: Effects of atmospheric modeling errors on estimates of baseline length, Radio

Acknowlegment:
This research has been supported by:
SMOG Project: PTDC/CTE-ATM/119922/2010;
PEst-OE/EGE/UI4056/2014ª UDI/IPG, funded by Foundation for Science and Technology